PAGEOPH, Vol. 144, Nos. 3/4 (1995) 0033–4553/95/040381–28$1.50 + 0.20/0

Analysis and Automatic Processing in Near-field of Eight 1992–1994 Tsunamigenic Earthquakes: Improvements Towards Real-time Tsunami Warning

F. SCHINDELÉ,[1] D. REYMOND,[1] E. GAUCHER[1] and E. A. OKAL[2]

Abstract—We study eight tsunamigenic earthquakes of 1992–1994 with data from single near-field 3-component long-period stations. The analysis is made from the standpoint of tsunami warning by an automatic process which estimates the epicentral location and the seismic moment through the variable-period mantle magnitude M_m. Simulations of early warning based on the real-time computation of the seismic moment are also tested with this system, which would give a justified warning in each region of tsunami potentiality. By exploiting the dependence of moment rate release with frequency, the system has the capability of recognizing both "tsunami earthquakes" such as the 1992 Nicaragua and 1994 Java events, as well as instances of the opposite case of low-frequency deficiency, interpreted as indicating a deeper than normal source (1993 Guam event). We report both the results of delayed-time processing of the near-field stations, and the actual real-time warnings at PPT, which confirm the former.

Key words: Tsunami, tsunami earthquakes, seismic moment, mantle magnitude.

Introduction

During 1992–1994, eight earthquakes generated measurable tsunamis in the Pacific and Indian Oceans and their adjoining seas (Table 1 and Figure 1a). Six of them, destructive and deadly, claimed a total of more than 2500 lives: Nicaragua (Sept. 2, 1992); Flores Sea, Indonesia (Dec. 12, 1992); Hokkaido (July 12, 1993); Java, Indonesia (June 2, 1994); Kuriles (Oct. 4, 1994); and Mindoro, Philippines (Nov. 14, 1994). The other two (Guam, Aug. 8, 1993; and Halmahera, Indonesia, Jan. 21, 1994) caused no casualties or damage directly attributable to the tsunami. This sudden recrudescence in tsunami activity, although most probably fortuitous, provides a rare opportunity to apply tsunami warning algorithms to a variety of earthquakes featuring significantly distinct tsunamigenic characteristics.

The seismic moment of these events was estimated in real time at the French Polynesia Tsunami Warning Center (Centre Polynésien de Prévention des

[1] Laboratoire de Détection et Géophysique et Centre Polynésien de Prévention des Tsunamis, Commissariat à l'Energie Atomique, Boîte Postale 640, Papeete, Tahiti, French Polynesia.

[2] Department of Geological Sciences, Northwestern University, Evanston, Illinois 60208, U.S.A.

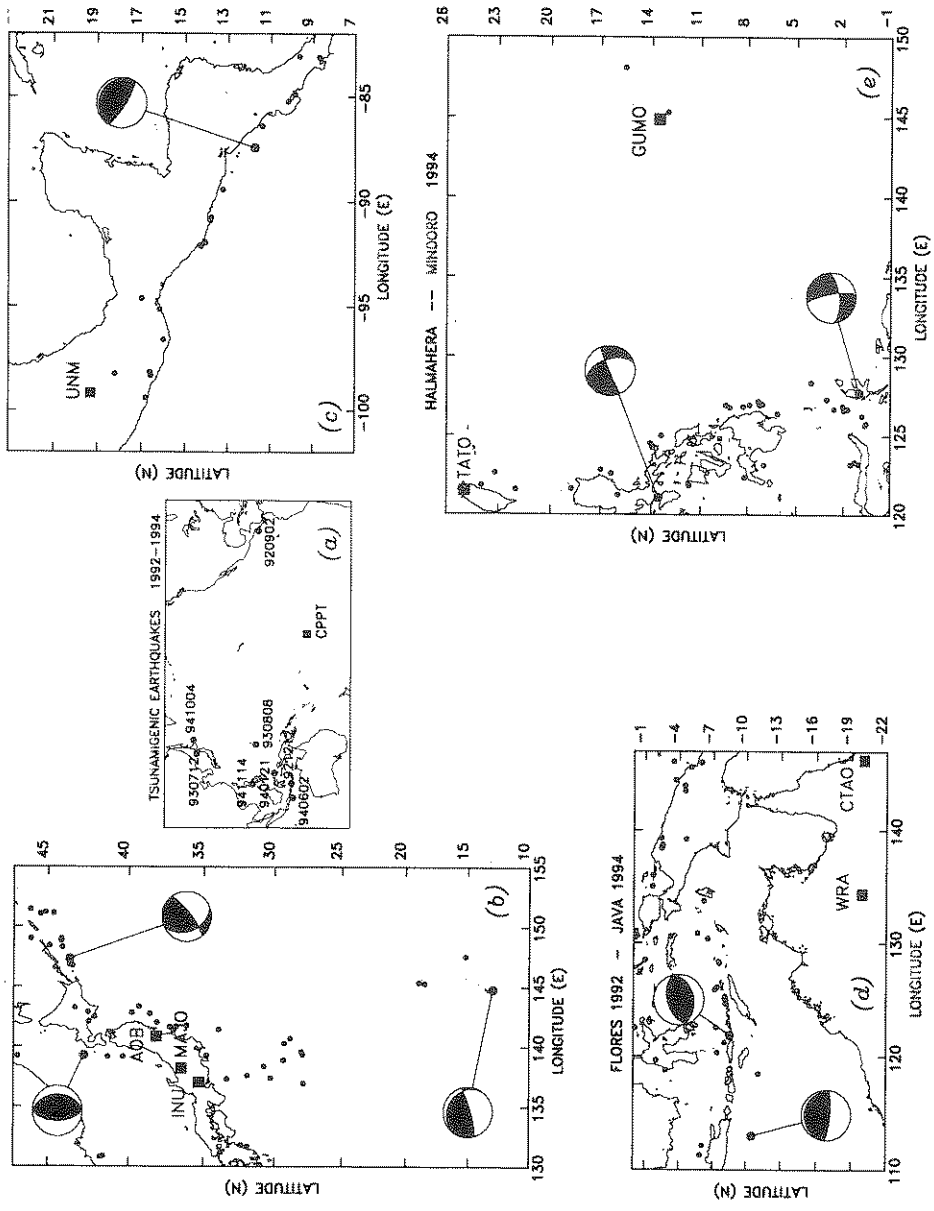

Figure 1

Maps of the eight tsunamigenic earthquakes studied in this paper (a): General map of the Pacific Ocean, showing the locations of the events (with date given as yymmdd), and of CPPT in Tahiti. (b–e): Close-up maps for each of the earthquakes under study. For each event, the CMT focal mechanisms are plotted with a solid line drawn to the exact epicenter. The station used in the near-field study is shown by a solid square. The background seismicity, extracted from the CMT catalogue (with $M_0 \geq 10^{19}$ N-m, and for the period starting in 1977 and ending before the earthquake studied) is shown as small solid circles. See text for details.

Table 1

Source parameters of the earthquakes studied

Date	Region	Epicenter °N	Epicenter °E	Depth (HRV; km)	m_b	M_s	Moment 10^{20} N-m
02 SEP 1992	Nicaragua	11.74	−87.34	10.0	5.3	7.2	3.4
12 DEC 1992	Flores Sea	−8.51	121.89	20.4	6.5	7.5	5.1
12 JUL 1993	Hokkaido	−42.84	139.25	16.5	6.7	7.6	4.7
08 AUG 1993	Guam	12.96	144.78	59.3	7.2	8.1	5.2
21 JAN 1994	Halmahera	1.01	127.73	15.0	6.2	7.2	0.32
02 JUN 1994	Java	−10.47	112.98	15.0	5.5	7.2	3.5
04 OCT 1994	Kuriles	43.71	147.33	59.0	7.4	8.1	37.
14 NOV 1994	Mindoro	13.57	121.08	15.0	6.0	7.1	0.59

Tsunamis, hereafter CPPT), and the estimates forwarded immediately to the National Earthquake Information Center and the Pacific Tsunami Warning Center. Ever since 1964, CPPT has been charged with the responsibility of issuing tsunami warnings (TALANDIER, 1993); the current procedure uses the automated algorithm TREMORS (**T**sunami **R**isk **E**valuation through seismic **MO**ment in a **R**eal time **S**ystem). This system, implemented at CPPT in 1987 (REYMOND *et al.*, 1991; HYVERNAUD *et al.*, 1992), is based upon the real-time estimation of the seismic moment through the variable-period mantle magnitude M_m (OKAL and TALANDIER, 1989), following the automatic detection and location of seismic events using a single three-component long-period seismic station.

The goals of the present paper are several: we report the actual results from CPPT, as they were obtained in real time following each of the eight earthquakes studied. We then use near-field records acquired after the fact, and processed through the TREMORS algorithm, in order to simulate and assess the performance of TREMORS in the near field, with respect to reliable and early warnings. We also test the accuracy of the automatic phase detection and epicenter location algorithm in the near field. We illustrate the significant advantage of a regional center equipped with this automated system, in the vicinity of each region with substantial tsunami risk. Finally, we confirm that two of the four largest tsunamis were due to so-called "tsunami earthquakes", i.e., events which generated disproportionate tsunamis in relation to their standard magnitudes; these earthquakes are characterized by a slow seismic moment release, evidenced by a steady increase in the spectrum of their seismic moment rate release with period.

Background

TREMORS is an integrated system based on a single three-component long-period seismic station which delivers a rapid early warning, a first location with

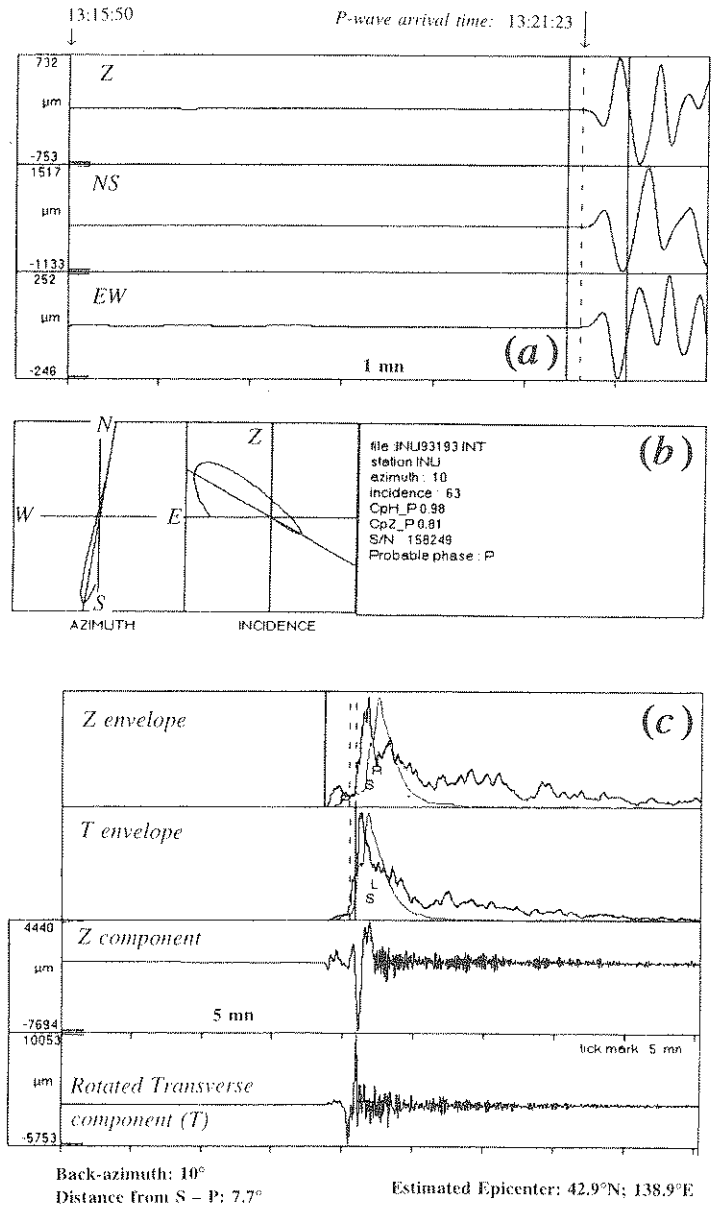
12 JULY 1993 (HOKKAIDO)
Station: INU
13:15:50
P-wave arrival time: 13:21:23
732
µm
-753
Z
1517
µm
-1133
NS
252
µm
-246
EW
1 mn
(a)
N
W
E
S
Z
AZIMUTH
INCIDENCE
file :INU93193.INT
station INU
azimuth : 10
incidence : 63
CpH_P 0.98
CpZ_P 0.81
S/N 158249
Probable phase : P
(b)
Z envelope
(c)
T envelope
4440
µm
-7694
Z component
5 mn
10053
µm
-5753
Rotated Transverse
component (T)
tick mark 5 mn
Back-azimuth: 10°
Distance from S – P: 7.7°
Estimated Epicenter: 42.9°N; 138.9°E

enough accuracy for immediate information and estimates of the seismic moment and tsunami risk. We give here a quick overview of the principal elements of the TREMORS algorithm, and refer the reader to REYMOND *et al.* (1991), for a more detailed description.

Location

The epicentral location is estimated from only two parameters: the $S - P$ time (or $R - P$ at short distances where the S and Rayleigh phases are often not well separated), and the back-azimuth best-fitting the polarization of P waves. This procedure is illustrated on Figure 2. These two parameters depend significantly on the signal-to-noise ratio, principally on the horizontal components, which can be noisy at long periods. Additionally, lateral heterogeneity in the earth on a global or regional scale can sway the ray outside of the expected great-circle plane. Our experience with teleseismic events recorded in Polynesia suggests an accuracy of 5° or better in azimuth when the horizontal signal-to-noise ratio (measured on energy) is 300 or more, and of 3° or better in epicentral distance when the signal-to-noise ratio on the horizontal instrument is at least 1000, these numbers relating to earthquakes at epicentral distances less than 107° (HYVERNAUD *et al.*, 1992).

Note that a *prelocation* can, in principle, be achieved immediately upon arrival of the P wave, by interpreting the angle of incidence of the P wave in terms of epicentral distance. However this procedure suffers from its sensitivity to crustal layering under the station, which in turn makes the result strongly frequency-dependent (see for example HASKELL (1962) for a discussion).

Estimation of the Seismic Moment

The seismic moment M_0 is estimated in realtime through the computation of the mantle magnitude M_m which was designed by OKAL and TALANDIER (1989) to obey the simple relation:

Figure 2

Automatic location procedure used by TREMORS, illustrated in the near field on the case of the Hokkaido earthquake recorded at Inuyama. (a) Close-up of the three-component seismogram showing the detection of the P wave. A 40-s fraction of time series (between the two vertical lines) is used in (b) to recover the back azimuth at the station (left) and the incidence angle of the arriving P wave (center). The latter could be used to compute a prelocation of the event, but note that the incidence angle is much less well constrained than the back azimuth. In (c), the horizontal records are then rotated using the back-azimuth information from (b), and the energy envelope of the transverse component used to detect the S_H arrival, which in turn yields the epicentral distance.

$$\log_{10} M_0 = M_m + 13.0, \tag{1}$$

where M_0 is in N-m.

We refer the reader to OKAL and TALANDIER (1989, 1990) and OKAL (1990) for the details of the computation of M_m, which is defined in the frequency domain as:

$$M_m = \log_{10} X(\omega) + C_D(\omega, \Delta) + C_S(\omega) - 0.90, \tag{2}$$

where $X(\omega)$ is the spectral amplitude of ground motion in μm-s at the angular frequency ω, C_S a source correction and C_D a distance correction. This formalism can be applied both to Rayleigh and Love waves with obviously different expressions for the corrections. Note that the source correction is in principle depth-dependent; in practice, corrections are computed for 4 broad bins of hypocen-

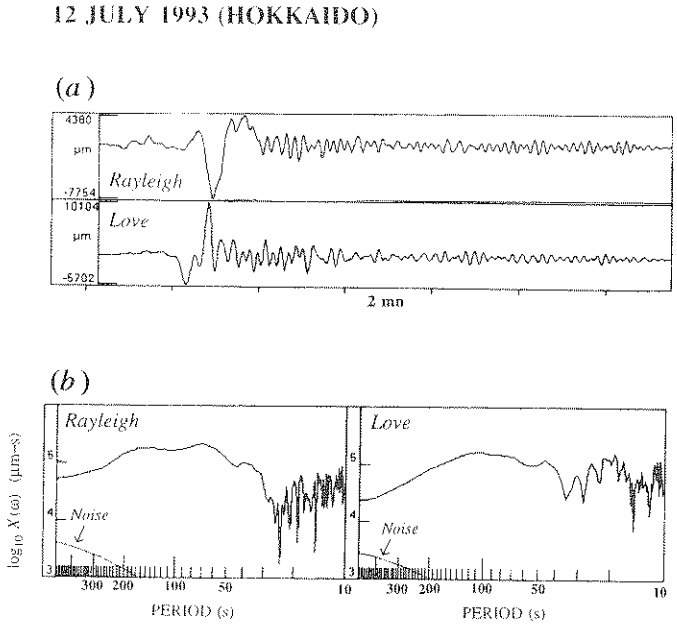

(c)

Period (s)	M_m	Moment (10^{20} N-m)
273.	7.82	6.61
256.	7.81	6.46
243.	7.82	6.61
183.	7.81	6.46
160.	7.81	6.46
142.	7.85	7.08
128.	7.88	7.59
116.	7.89	7.76
107.	7.90	7.94
98.	7.90	7.94
85.	7.91	8.13
75.	7.90	7.94
67.	7.93	8.51
61.	7.92	8.32
56.	7.89	7.76
51.	7.89	7.76

Figure 3

Automatic computation of mantle magnitude M_m and estimation of seismic moment M_0 by the TREMORS algorithm, illustrated in the near field on the case of the Hokkaido earthquake recorded at Inuyama. (a): Time series used in the final analysis (the Love wave trace has been offset for clarity due to difference in group velocities. (b): Raw spectra (in logarithmic scale) of the above records, before the distance and source corrections have been applied. The smaller trace in the bottom left corner represents the level of background noise, obtained by processing a window of similar duration occurring prior to the event. (c): Ouptut of the computed values of M_m and corresponding estimations of M_0 obtained from the Rayleigh spectrum.

tral depths (OKAL, 1990). In the case of Rayleigh waves at teleseismic distances ($\Delta \geq 10°$), M_m can also be computed directly in the time domain (OKAL, 1989).

In practice, the computation of the seismic moment can be initiated when a few minutes of surface waves have been recorded by the system (15 minutes or more in the absence of emergency). This procedure is illustrated on Figure 3. The computer systematically calculates M_m from Rayleigh waves for each category of focal depth (and from Love waves for a shallow source), and prints the results, with an operator on call 24 hours a day, having the final responsibility of deciding the most plausible depth. Further development is presently being undertaken to attempt to recognize automatically a deep focus (and eliminate it from the standpoint of tsunami danger), based on the combination of the incidence angle of the P wave, and of the total duration of the signal (which would discriminate against a teleseismic event with the same incidence angle).

Results compiled on a dataset of 474 earthquakes during the years 1987–91, and expressed through the residual

$$r = M_m(\text{measured}) - \log_{10} M_0(\text{published}) + 13 \tag{6}$$

feature an average $\bar{r} = 0.07$ units of magnitude, and a standard deviation $\sigma = 0.22$ units (HYVERNAUD *et al.*, 1992). The quality of these results is comparable to that shown in previous studies from OKAL and TALANDIER (1989) and REYMOND *et al.* (1991). In the near field ($1.5° \leq \Delta \leq 15°$), an analysis made on a dataset of 115 records from shallow earthquakes yields $\bar{r} = 0.17$; $\sigma = 0.29$ units (TALANDIER and OKAL, 1992). These results express the excellent performance of the mantle magnitude M_m, as an estimator of the seismic moment M_0.

Tsunami Warning

● *P-wave warning:* Two warning systems are in effect at CPPT; a classical warning system is based on the amplitude of P waves, measured on a broad-band record, with a triggering threshold fixed at 100 μm. For a regular earthquake whose source time behavior approaches a step function, this corresponds approximately to a moment of 10^{20} N-m at typical teleseismic distances. However, this first warning can occasionally be deficient, since body waves are a poor descriptor of the long-period properties of the source: for example, in the case of the 1992 Nicaragua and 1994 Java earthquakes, the triggers were activated at PPT neither on the short-period nor on the long-period channels (also, false alarms could indeed be generated by deep earthquakes with strong P waves). Nevertheless, the warning based on P waves, when triggered, does retain some value, given that it is available as soon as the arrival time of P waves.

It would be inappropriate to lower the P wave warning threshold in order to trigger on slow, "tsunami", earthquakes, since this would result in the issuance of

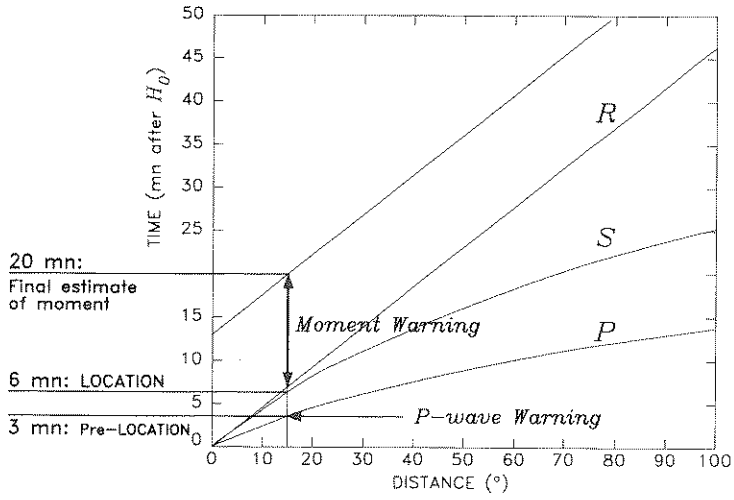

Figure 4

Time delay of P and M_0 warnings as a function of epicentral distance. The travel-time curves of P, S and the Airy phase of the Rayleigh wave (R) are plotted for a shallow earthquake. The fourth curve is obtained as ($R + 13$ mn). The case of $\Delta = 15°$ is highlighted: the P phase arrives 3 mn after origin time, triggering a P warning if the threshold is exceeded. The location is computed at the time of the S arrival (6 mn at 15°), and the seismic moment can exceed the assigned threshold anytime (generally a few minutes) after the R arrival. The final estimate of the moment is given 20 mn after H_0.

warnings for all earthquakes above approximately $m_b \geq 5.8$, most of which carry no tsunami danger. For this reason, the TREMORS warning is based on an estimate of the seismic moment. It is clearly superior as a tsunami warning, even though it only becomes available at a later time (see Figure 4).

● *TREMORS warning:* Once the seismic moment of the earthquake is computed, the tsunami warning proceeds from the observation that the amplitude of a tsunami on the high seas at teleseismic distance from the source is a linear function of the moment of the parent earthquake. This was both derived theoretically (OKAL, 1988), and verified experimentally on the basis of a dataset of 17 tsunamis at Papeete (TALANDIER and OKAL, 1992). In particular, we have argued in OKAL (1988) that the precise value of hypocentral depth (as long as $h \leq 70$ km), and the geometry of the focal mechanism have only minor influences on the amplitude of teleseismic tsunamis. In the near field, such effects are expected to become more important; however, the seismic moment M_0 remains the crucial seismological parameter controlling tsunami excitation.

The warning threshold at CPPT is fixed at 1.0×10^{20} N-m and six of the eight earthquakes under study generated a seismic moment warning, fifteen minutes after the Rayleigh arrival. As detailed in TALANDIER and OKAL (1989), various levels of warning (watch, alarm, etc.) have been defined as a function of the estimate of M_0, and of the particular epicentral region, in relation to Polynesia. It is clear that, in the context of a regional warning system, the warning threshold for M_0 would have

Table 2

PPT Real-time results

Event	USGS Location Δ (°)	USGS Location Back azimuth (°)	TREMORS Δ (°)	TREMORS Back azimuth (°)	M_m	Moment (10^{20} N-m)
Nicaragua	68.1	69.2	69	71	7.5	3.2
Flores	86.0	262.4	90	261	7.9	8.0
Hokkaido	88.8	315.9	93	305	8.0	10.0
Guam	71.6	290.6	73	283	7.95	9.0
Halmahera	83.3	273.2	96	272	6.9	0.87
Java	93.8	257.8	90	250	7.4	2.5
Kuriles	83.9	319.4	83	321	8.3	20.
Mindoro	93.4	283.0	94	275	7.3	2.0

to be adapted regionally, notably through the use of available runup and inundation maps for documented historical tsunamis.

Real-time Results at CPPT for the 1992–94 Tsunamis

Table 2 summarizes the parameters obtained in real time by the TREMORS algorithm running at CPPT. In all instances, these parameters were forwarded to the appropriate agencies (NEIC, PTWC) within one hour of the earthquake's origin time. In several cases, they are believed to have been the first estimates of the earthquake's seismic moment to be made available. However, in all cases, the large epicentral distances for PPT restricted the tsunami risk for Polynesia. In addition, in several cases, the tsunami occurred in seas with little if any opening into the main Pacific Ocean, actually alleviating the teleseismic risk totally.

The residuals in distance to PPT (true distance − distance evaluated by TREMORS) vary between $-13°$ (in the case of the small Halmahera event; otherwise $-4°$) and $+2°$, and the residuals in azimuths between $-2°$ and $+10°$. In a few instances, the accuracy of the TREMORS solution is insufficient to assess whether the epicenter is under the ocean, or under a continental mass or a large island. Yet, it is always sufficient to estimate the seismic moment in real time. A comparison between the moments obtained at PPT and later published by the Harvard group (DZIEWONSKI *et al.*, 1993a,b, 1994a,b; G. Ekström, pers. comm., 1994) shows that the TREMORS estimates are within a factor varying from 0.7 to 2.1 of the final CMT solutions, corresponding to an error on the mantle magnitude varying between -0.15 and $+0.32$ units (Figure 5). To put these numbers in perspective, it is useful to remember the general scatter of the estimates of

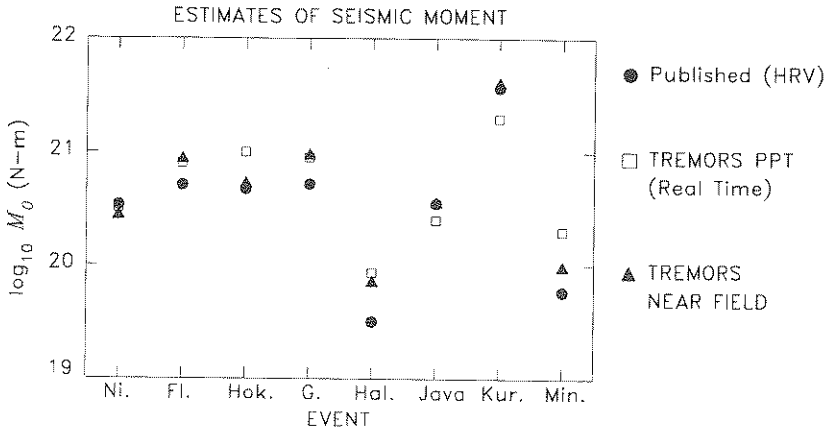

Figure 5
Comparison of the moment values obtained from CMT inversion by the Harvard group (solid circles) for each of the eight earthquakes studied, with estimates obtained in real time at PPT (open squares), and near-field estimates obtained with the TREMORS algorithm in the present study (solid triangles).

conventional magnitudes which are given in the hours immediately following a large earthquake.

Near-field Results

In a previous study, TALANDIER and OKAL (1992) demonstrated the validity of the mantle magnitude algorithm at regional distances down to 1.5° for the purpose of estimating the seismic moment of an event. However, their study required the knowledge of the exact epicenter, and as such was an after-the-fact exercise. In the context of TREMORS, it is necessary to investigate the performance of the method in providing in real time a reasonable estimate of the epicenter, from which the quantification of the source can proceed. We have recently adapted the TREMORS software to the particular case of near-field warning, for which the minimization of response times is crucially important. In order to avoid the pitfalls of classical warning systems which use a simple criterion based on P-wave amplitudes, TREMORS proceeds through a real-time computation of the seismic moment, which we will now briefly describe.

As the various phases composing the seismic signal are received at the station, a dataset of increasing duration is used for the determination of the seismic moment: this window is regularly increased in steps of 50 s, until mantle waves with the longest periods (300 s) have been included. This procedure is illustrated on Figure 6. The presumed location of the earthquake, which is necessary to estimate

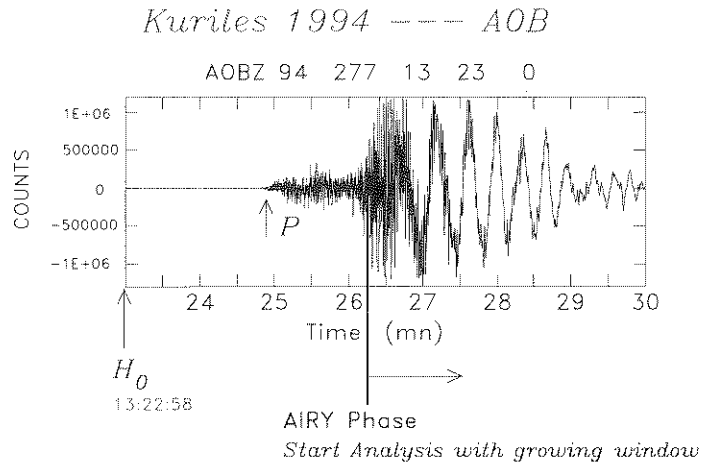

Figure 6

Broadband record at Aobayama, Japan (AOB) of the great 1994 Kuriles earthquake. This figure illustrates the computation of M_m using a growing window: the computation starts upon arrival of the Airy phase (around 13:26:30 GMT); the beginning of the windows remains constant, but their durations are progressively increased in steps of 50 s.

the seismic moment, is calculated from its back azimuth (obtained from the polarization of P waves at trigger time), and distance (itself obtained from the identification of S in the growing window; at short distances, S and Rayleigh waves may not be differentiated). Once the location is estimated, the signal is Fourier-transformed, the magnitude M_m computed, and the seismic moment estimated, at each of the Fourier periods between 50 and 300 s. If the seismic moment is greater than the established threshold, a warning is sent automatically by the computer. This procedure is repeated regularly as more data become available, which in practice allows the study of the source at increasingly longer periods. However, the main advantage of the growing window is to minimize the response time of the algorithm, by allowing the issuance of a warning even before the longest periods have been received, should the characteristics of the early wavetrains warrant it. This point becomes crucial to an efficient warning system, as the epicentral distances are reduced, and will be particularly important in the case of the Kuriles event (see below).

For each of the eight tsunamis, we acquired very-broad-band data from stations located as close as possible to the relevant epicenters, and processed the datasets through the TREMORS automatic software (Table 3). Although conducted in delayed time, our experiment represents a test of the real-time performance of TREMORS, had the system been operational at a regional station. In practice, we use IRIS GEOSCOPE and POSEIDON Very Broad Band (VBB) channels. We refer to the IRIS annual reports, and to ROMANOWICZ *et al.* (1984), respectively,

Table 3

Near-field results

Event	Station	USGS Location Δ (°)	USGS Location Back azimuth (°)	TREMORS Δ (°)	TREMORS Back azimuth (°)	M_m	Moment (10^{20} N-m)
Nicaragua	UNM	13.7	121.9	15	133	7.4	2.7
Fores	CTA	26.2	292.6	27	290	7.9	8.6
Hokkaido	INU	7.7	12.3	7.7	11	7.7	5.2
Guam	MAJO	24.2	164.2	23	167	8.0	9.3
Halmahera	GUMO	21.0	235.1	22	240	6.85	0.7
Java	WRA	22.6	291.4	24	289	7.55	3.5
Kuriles	AOB	7.33	39.9	8.1	45	8.6	40.
Mindoro	TATO	11.4	182.0	11.4	187	6.98	0.95

for a description of the networks, including the instrument responses at mantle wave periods. Despite the occasionally low sampling rate of some channels (10 s), the location algorithm performed well, as will be discussed in detail below.

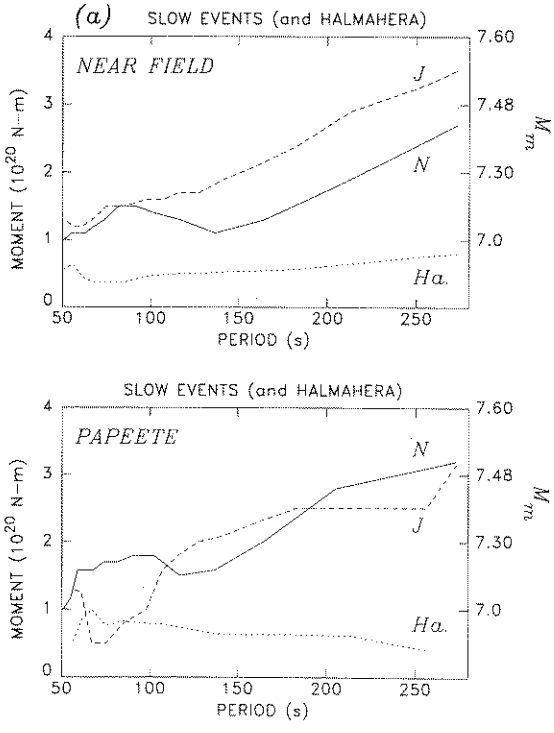

Figure 7(a).

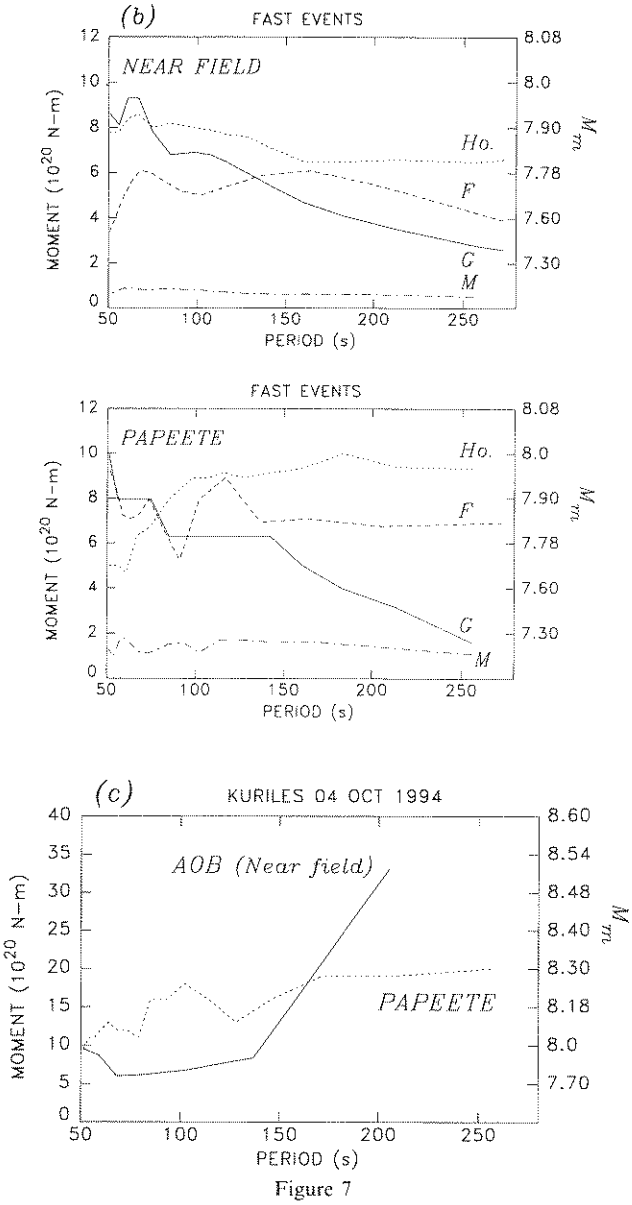

Figure 7

Value of the seismic moment M_0 obtained from TREMORS as a function of period. This quantity is equivalent to the spectral amplitude of the rate of moment release. These values are taken from the final window of analysis. The data has been split into (a) slow events ("tsunami earthquakes") and Halmahera; and (b) fast events. The Kuriles earthquake is plotted separately (c) due do its size. In (a) and (b), we plot separately the results at Papeete, and for the near-field station selected. In the case of Nicaragua (N) and Java (J), note the regular increase in seismic moment with period, indicative of a slow source. On the other hand, in the case of Hokkaido (Ho.) and Flores (F), the spectrum is fundamentally flat. Note that in the case of the Guam earthquake (G), the moment actually *decreases* with period.

We refer to the abundant existing literature, including the other papers in this volume, for complete descriptions of the events under study. For each of them, we will emphasize only the features most important from the standpoint of their tsunami generation, and proceed to discuss in detail the estimates of seismic moment and tsunami risk provided by our automated algorithm.

The earthquakes are presented in chronological order, except for the small Halmahera event, which is discussed last on account of its much smaller moment and tsunami.

● *Nicaragua, 1992*

The earthquake occurred on September 2, 1992 at 00:16 GMT, and was barely felt by residents along the coast of Nicaragua (Figure 1c). Its intensity was mostly II along the coast, and reached III only at a few places. Forty to seventy minutes after origin time, the tsunami reached the coast, with amplitudes of 4 m above the ambient sea level in most places along a stretch of 200 km of coastline, and a maximum runup height of 10.7 m (SATAKE *et al.*, 1993). The death toll, entirely due to the tsunami, was around 170.

The nearest broadband station from which we obtained data is the GEOSCOPE station UNM in Mexico City, at a distance of 13.7° from the epicenter. The TREMORS epicentral location is at {8.8°N, 88.1°W}, corresponding to errors of 1.3° in epicentral distance and 11.1° in azimuth. The latter is surprisingly large, and is probably due to a path refracted along the slab (based on numerous surface wave polarization studies, LASKE (1995) has shown that the orientation of the sensors at UNM is indeed very good, so that the effect of their misalignment can be dismissed). The TREMORS epicenter is situated in the Pacific continental margin, which is sufficient to warrant a warning for all the Pacific coasts of Nicaragua and Costa Rica. The seismic moment estimate (2.7×10^{20} N-m) is in good agreement with the Harvard CMT value (3.4×10^{20} N-m). The seismic moment rate spectrum shows a first peak (1.5×10^{20} N-m) at 70 s, followed by a slight decrease (to 1.0×10^{20} N-m) until 140 s (Figure 7a); beyond 140 s, the seismic moment increases rapidly, reaching 2.7×10^{20} N-m at 273 s. The large increase in the size of this event with period suggests a long source process, as independently demonstrated by many other studies (e.g., KANAMORI and KIKUCHI, 1993), and this event must be classified as a "tsunami earthquake," as confirmed by the large $m_b : M_s$ and $M_s : M_0$ discrepancies (Table 1).

● *Flores Sea, 1992*

On December 12, 1992 at 05:29 GMT, a very strong earthquake struck the eastern region of Flores Island (Figure 1d) and caused substantial damage and casualties. Because the rupture zone was very close to the coast, the tsunami

attacked the coastal area within 5 minutes of the earthquake. KAWATA (1993) reveals that the residents had no information on tsunamis, so at the time of the earthquake, no one ran away from the shores. The tsunami had an average runup of 3 m, and a maximum height of 26 m was documented at the site of the village of Riangkrok, which was totally wiped out (YEH, 1993). This huge tsunami also attacked the southernmost part of Sulawezi Island, where it caused 22 deaths and damaged more than 400 buildings (SUNARJO, 1993); it reached Ambon-Baguala Bay on Ambon Island two hours after the earthquake.

The nearest station for which we obtained data is the IRIS station at Charter Towers, Australia (CTA), a distance of 26.2° from the epicenter. The TREMORS location is 150 km from the epicenter, with an error of 0.8° in distance and 2.6° in azimuth. This level of accuracy is insufficient to determine whether the earthquake is south of Flores Island, in the open Indian Ocean or North of the island, in the closed Flores Sea. The seismic moment is estimated at 8.6×10^{20} N-m, somewhat larger than the Harvard CMT value (5.1×10^{20} N-m). As shown on Figure 7b, the moment release remains very stable between 50 and 100 s, and then decreases slowly at periods larger than 150 s. Several factors did contribute to the exceptional amplitude of the tsunami waves, relative to the seismic moment: in addition to the general vicinity of Flores Island to the rupture zone, and to the shallow water depth in the epicentral area (only about 1000 m), it is probable that underwater landslides took place in the neighborhood of the highest observed runup, at the extreme northeast end of the island of Flores.

● *Hokkaido-Nansei-Oki, 1993*

This earthquake took place at 13:17 GMT on July 12, 1993 (Figure 1b), and was widely felt throughout Hokkaido, Northern Honshu and the neighboring islands. Two to five minutes later, the tsunami devasted Okushiri Island, then hit Hokkaido; the total loss of life was upward of 200. We refer to FURUMOTO (1993) and NAKANISHI *et al.* (1993) for a complete description of this earthquake and tsunami. Runup heights were an average of 5 m on Okushiri, reaching up to 30 m on the southwestern coast of the island (HOKKAIDO TSUNAMI SURVEY GROUP, 1993). Wave heights of more than 7 m were reported along Hokkaido's coasts; in 50 to 70 minutes, the tsunami crossed the Sea of Japan and reached the Russian and Korean coasts, with average runup heights of 2 m, reaching up to 4 m at some locations. The rupture zone of the earthquake reached within a few km of Okushiri Island, which explains both the short time interval between earthquake and tsunami, and the very large runup heights (TANIOKA *et al.*, 1993).

The nearest station for which we obtained data is GEOSCOPE station INU at Inuyama, Japan, a distance of 7.7° from the epicenter. The TREMORS location based on this station is {42.9°N, 139.1°E}, 30 km from the epicenter, the distance being correct and the azimuth 1.3° off. The TREMORS epicenter is located very

close to the actual epicenter and a warning for all coastal areas of the Sea of Japan (Hokkaido, Honshu, Russia, Korea) would be possible with this location.

Several factors contributed to the very large amplitude of the tsunami waves for this event, relative to its seismic moment: in addition to the extreme vicinity of the source from Okushiri Island, the reduced water depth (typically on the order of 1000 m in the epicentral area) enhanced significantly the tsunami excitation.

● *Guam, 1993*

On August 8, 1993, at 08:34 GMT, a powerful earthquake occurred near Guam (Figure 1b) causing extensive damage and injuring more than 50 people on the island of Guam. The event generated tsunami waves of 30 cm to 1 m amplitude recorded at tidal stations in Southern Japan.

The nearest station for which we obtained data is MAJO, the IRIS station at Matsushiro, Japan, a distance of 24.2° from the epicenter (power failure throughout

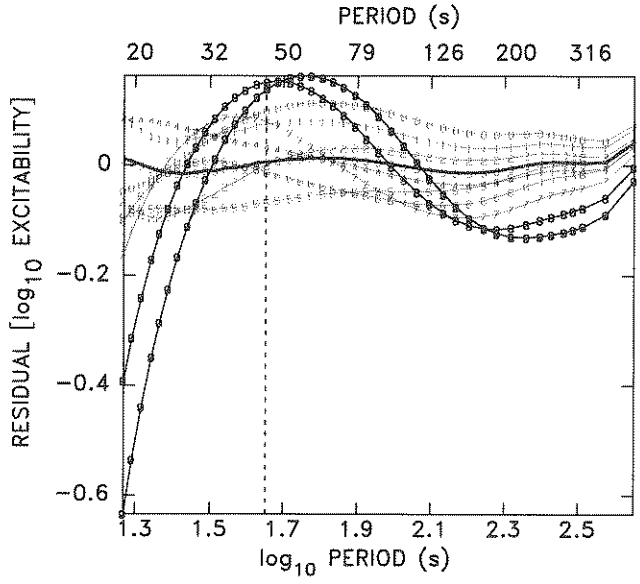

Figure 8

Residual of the logarithmic average excitability as a function of period for several depths of shallow earthquakes, after TALANDIER and OKAL (1989). For each depth (labeled 0 to 9 and extending from 0 to 75 km), the trace represents the average error introduced by using the correction C_S, instead of a proper excitability, in the computation of M_m. C_S is designed to model the excitability at 20 km (3; thick, nearly horizontal trace). Note that for depths of 60 (8) and 75 km (9), the excitability is larger than modeled at 50 s, but becomes smaller at the mantle periods (150–250 s). Accordingly, the magnitude of the event is overestimated (by about 0.15 units) at 50 s, and underestimated (by about 0.15) at 200 s. The decrease in magnitude (of about 0.3 units) between 50 and 200 s can therefore be an artifact of a deeper than usual source.

the island of Guam knocked down station GUMO at what should have been trigger time). The TREMORS location is {13.9°N, 143.3°E}, about 185 km from the epicenter, with an accuracy of 1.2° on the distance, and 2.8° on the azimuth. The TREMORS epicenter is situated in the Parece-Vela Basin, which is sufficient for a warning for the western coasts of the Marina Islands and the southwestern coasts of Japan.

The seismic moment estimated is 9.3×10^{20} N-m, significantly larger than the Harvard CMT value (5.2×10^{20} N-m). It is remarkable that this estimate is obtained at a period of 67 s, and that the surface wave seismic moment rate spectrum is peaked around 60–70 s, followed by a steady decrease to 2.5×10^{20} N-m at 273 s (Figure 7b). In order to compare more significantly our solution with the Harvard CMT value, we should use the estimate of the seismic moment at the period (135 s) used exclusively in the latter. The agreement (5.8×10^{20} as opposed to 5.2×10^{20} N-m) then becomes excellent.

The unexpected shape of the moment release rate spectrum for the Guam earthquake is due to its significant hypocentral depth (60 km, while most other sources are shallower than 20 km). As shown on Figure 8 (from OKAL and TALANDIER, 1989), which plots the logarithmic average excitability of Rayleigh waves for a combination of frequencies and source depths, hypocenters at 60 to 75 km (8 and 9 on the figure) exhibit maximum residual excitation (computed relative to $h = 20$ km) around 50 s, followed by a decrease of 0.3 orders of magnitude down to 200 s. The correction for the true hypocentral depth and focal mechanism of the event amounts to 0.4 orders of magnitude, and brings the moment in close agreement with the Harvard CMT value.

● *Java, 1994*

On June 2, 1994, at 18:18 GMT, a major earthquake took place in the Java trench about 200 km southeast of Malang (Figure 1d). Forty to sixty minutes after the earthquake, a tsunami hit the southern coast of Java, killing at least 250 people, and inflicting considerable damage. Tsunami runup heights averaged 4 m, and exceeded 11 m at several locations.

The nearest station at which we obtained data is WRA, the IRIS station at Warramunga Array, Australia, a distance of 22.6° from the epicenter. The TREMORS location (10.6°S, 111.4°E) is 125 km from the actual epicenter with an accuracy of 1.4° in distance and 2.4° in azimuth. The TREMORS epicenter is located in the Indonesian Trench, which is sufficient to warrant a warning for all the southern coast of Java and adjoining islands. The estimate of the seismic moment, 3.5×10^{20} N-m, is the same as the Harvard CMT value. The seismic moment rate spectrum shows a large and continuous increase in amplitude with period, from 1×10^{20} at 50 s to 3×10^{20} N-m at 273 s (Figure 7a). This large increase in amplitude suggests a long source time function, and this event must be

classified as a "tsunami earthquake." Significant aerial landslides were observed in the eastern portion of Java, suggesting that underwater ones may also have taken place.

● *Kuriles, 1994*

This very large earthquake occurred on October 4, 1994 at 13:22 GMT, approximately 80 km from the islands of Shikotan and Iturup, in the Southwestern Kuriles. With a preliminary CMT moment of 3.7×10^{21} N-m, this event is the largest earthquake recorded worldwide since 1977, and possibly 1965 (KANAMORI, 1977). It generated a Pacific-wide tsunami, which prompted evacuation of certain coastal areas, notably in Hawaii. Local runup heights reached 9 m on Kunashir and Shikotan Islands. It is unclear if any of the 11 reported deaths were attributable to the tsunami.

The event was located by CPPT at {44°N, 150.5°E}, 250 km away from the true epicenter, an error of only 1.4° in distance, and 2° in azimuth. This location, and the moment (2×10^{21} dyn-cm) obtained at CPPT, predict a Pacific-wide tsunami, albeit one with only moderate amplitude; this explains that a warning, but no alarm, was issued for Polynesia. The amplitude at Papeete harbor was 23 cm.

The closest station for which we obtained data is the POSEIDON station at Aobayama, Japan (AOB), a distance of 7.3°. TREMORS located the event about 110 km west of the true epicenter, and yields a moment of 4×10^{21} N-m, in excellent agreement with the preliminary Harvard CMT value. There is some suggestion of an increase of M_m with period, which may reflect the source duration (70 s according to the preliminary CMT, a figure in general agreement with the size of the event), and offset the effect of source depth (50 to 60 km).

● *Mindoro, Philippines, 1994*

This relatively small event took place on November 14, 1994 at 19:15 GMT in the immediate vicinity of the coastline of Mindoro (at the time of writing, it is still unclear if the epicenter was on land or at sea; C. E. SYNOLAKIS, pers. comm., 1994). It generated a local tsunami in the Bay of Marinduque, with runup heights of up to 6 m on Mindoro, resulting in approximately 70 deaths. Because of the combination of a large epicentral distance (94°), and of the relatively poor signal-to-noise ratio, the TREMORS location at CPPT is significantly offset (8.2° in back azimuth) from the true epicenter.

The nearest station for which we obtained broadband data is TATO, the IRIS station at Taipei, Taiwan, a distance of 11.4° (Figure 1e). The solution obtained, {13.60°N; 120.07°E}, is about 250 km from the true epicenter, on the Palawan shelf. The seismic moment, 9.5×10^{19} N-m, is about 1.6 times the preliminary CMT solution. The spectrum of the moment release rate is essentially flat.

● *Halmahera, 1994*

Finally, and despite its much smaller size, we discuss the case of Halmahera event of January 21, 1994: it will allow us to get insight into a reasonable threshold for tsunami warning in the near field. At 02:04 GMT, a strong earthquake struck Halmahera Island (Figure 1e), killing 9 people and causing extensive damage to that Indonesian island. Minor tsunami waves, with a maximum runup of 2 m, were reported on its western coast. No deaths or significant damage were attributable to the tsunami.

The nearest station for which we obtained data is GUMO, the IRIS station at Agaña, Guam, a distance of 21.0° from the epicenter. The TREMORS epicenter (1.9°N, 126.0°E) is 210 km from the actual focus, with an accuracy of 1.0° in distance and 4.9° in azimuth. The seismic moment estimate is 7.3×10^{19} N-m, with the moment rate release spectrum basically flat from 50 to 250 s. The difference with the Harvard CMT value (3.2×10^{19} N-m) can be accounted for by the particular orientation of the station with respect to the focal mechanism. The low value of M_0, which is adequately recognized by TREMORS, explains the relatively benign character of the tsunami, and suggests that this range of moments constitutes the limit for the generation of destructive tsunamis in the near field.

Discussion

At this point, and based on our results for the eight earthquakes studied, we confirm TALANDIER and OKAL's (1992) result, namely that M_m performs flawlessly in the near field. In particular, a comparison between near-field results and the value computed for the same events at PPT confirms the validity of our estimates. In addition, we show that our detection algorithm is usually reliable at those short distances, indicating that the whole TREMORS software yields acceptable estimates of the seismic moment in real time (within ± 0.3 orders of magnitude for the present dataset), thus reaching a new milestone for efficient tsunami warning. Even in the case of a poor epicentral solution (Mindoro as located by TATO), the estimate of the seismic moment remains acceptable.

Beyond the mere estimation of seismic moment, it is particularly important to discuss the ability of TREMORS to recognize exceptional features of the earthquake source, and to do so in real-time. Among the eight earthquakes considered, the following characteristcs are of particular interest for tsunami warning:

* the character of the event as a "tsunami earthquake" (Nicaragua, Java), i.e., the existence of a slow source time function;
* the case of a truly large seismic moment (Kuriles); and
* the case of an earthquake of very large conventional magnitude generating only a benign tsunami (Guam), presumably due to its source depth.

We show here that TREMORS does recognize all these characteristics, and can do it in real time.

Anomalous Seismic Moment Rate Spectrum for Tsunami Earthquakes

As shown on Figure 7b, the moment spectra characteristics of the Flores, Hokkaido and Mindoro earthquakes correspond to a typical source time function, which cannot be distinguished from a step-function moment release at periods greater than 50 s. On the other hand, the Nicaragua and Java spectra (obtained both in near field and at PPT) feature an increase of about 0.4 orders of magnitude in the seismic moment rate spectrum from 50 to 273 s. This situation is particularly well expressed in the case of the Nicaraguan event, as analyzed at UNM with the growing time window: the first available estimate of the seismic moment is barely 10^{19} N-m, and this value grows by a factor of 20 over five minutes of elapsed time. In contrast, in the case of the Flores earthquake, the estimate of M_0 grows only by a factor 3. Figure 8 shows that this cannot be attributed to an artifact of source depth for shallow earthquakes; hence the Nicaragua and Java events are "tsunami earthquakes" with anomalous source properties leading to extended source durations. In terms of phenomena responsible for this behavior, leading contenders would be rupture velocities significantly slower than the commonly assumed 2.5 to 3.5 km/s, themselves a probable reflection of the influence of sedimentary structures in the immediate vicinity of the source (KANAMORI and KIKUCHI, 1993; TANIOKA and SATAKE, 1994). In turn, such structures may enhance tsunami excitation relative to seismic waves, and beyond its value expected on the basis of the zero-frequency value of the moment, as documented theoretically by OKAL (1988). Thus it is particularly important that TREMORS cannot only obtain the final static moment, but also document the slow character of the source.

The Case of a Truly Large Earthquake: Kuriles

In the case of the Kuriles event, the very first measurement obtained at station AOB, 4 minutes after origin time, is already in excess of 10^{21} N-m. While the final value, obtained a few minutes later grows to 4×10^{21} N-m (mainly due to the dimensions of the source), it becomes immediately clear that one deals with a major earthquake, which will generate a major tsunami, regardless of the values obtained later, and an alarm can be issued as early as 4 mn after origin time. This illustrates the power of our algorithm which begins computing estimates of M_0 immediately upon arrival of the Airy phase.

The Case of a Tsunami-deficient Event: Guam

Finally, in the case of the Guam earthquake, the strong decrease of moment rate spectra with period (Figure 7b) reflects the significant depth of the event (60 km);

as detailed above (and on Figure 5), the moment is overestimated (by about 0.4 units of magnitude) at the shorter periods, because of the particular behavior of the excitability of Rayleigh waves at 60 km. The low-frequency M_0 obtained by TREMORS is in excellent agreement with the CMT solution, and explains the relatively benign tsunami, despite a conventional surface wave magnitude $M_s = 8.1$. It is important to note that TREMORS can be used to recognize this property in real time by monitoring the evolution of M_0 with period. The only alternative explanation would be to seek a source time function deficient in low frequency with respect to a step function, which is improbable (it would require a significant rollback), and at any rate would not favor tsunami generation. We also note that a more stable rate of moment release is obtained if the earthquake is processed as having intermediate depth; however, the depth of the earthquake could not be determined independently in real time because of the difficulty of using automated algorithms for depths less than 150 km, due to the interference between pP and P on long-period records.

m_b vs. M_0: A Possible Identifier of Slow Earthquake Sources

In this section, we investigate the relationship between the body-wave magnitude m_b and the seismic moment M_0 as a possible means of identifying "tsunami

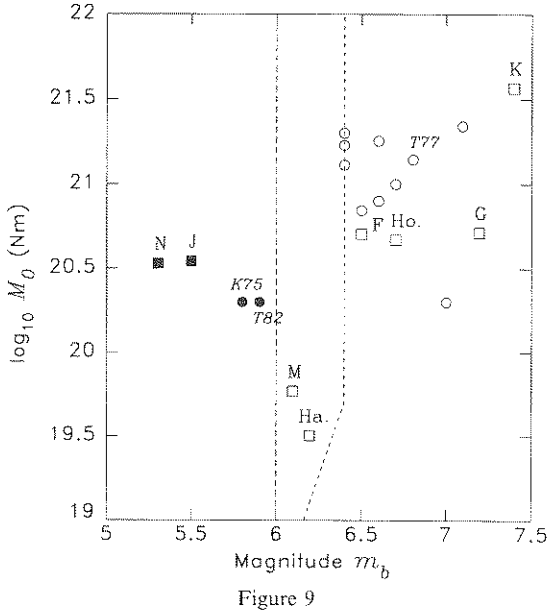

Figure 9

Comparison of m_b and M_0 values for a number of tsunamigenic earthquakes of the past 30 years (see Table 4). The eight events in the present study are shown as squares. "Tsunami earthquakes," exhibiting strong $m_b : M_0$ deficiencies are shown by solid symbols. The vertical long-dashed line is the $m_b = 6$ saturation level in the model of GELLER (1976). The segmented line with shorter dashes follows the model of OKAL and ROMANOWICZ (1994).

earthquakes" in real time. When first describing "tsunami earthquakes," KANAMORI (1972) suggested that they result from an anomalously long source time function, which causes a large discrepancy between the seismic moment M_0 and its value expected from the conventional magnitude M_s, computed at higher frequency. This was later confirmed by a number of scientists who based most of their studies on a comparison between M_s and various seismic parameters (M_0, tsunami height, etc.).

In the present study, we elect to focus on the relationship between m_b and M_0 for a number of reasons. First and foremost, from an operational standpoint, m_b can be computed as early as the arrival time of S waves (the knowledge of $S-P$ is necessary to compute the distance correction), and does not require waiting for surface waves. Thus, and however incomplete and possibly misleading it may be, m_b remains the first available estimate of the size of the earthquake; on the other hand, as soon as the surface waves have arrived and M_s can be computed, the more significant M_m becomes available, and thus there is no advantage at this point in evaluating M_s for the purpose of quantifying the earthquake source.

It is well known (e.g., GELLER, 1976) that the magnitude scale m_b saturates around 6.0 to 6.5 (when properly measured at 1 s), but this saturation can actually

Table 4

Parameters of earthquakes used in Figure 9

Data	Region	m_b	M_s	M_0 (10^{20} N-m)	Symbol on Figure 9
17 OCT 1966	Peru	6.4	7.5	20	
11 AUG 1969	Kuriles	7.1	7.8	22	
17 JUN 1973	Japan	6.5	7.7	7	
03 OCT 1974	Peru	6.6	7.6	18	
10 JUN 1975	Kuriles	5.8	7.0	2	K75
22 JUN 1977	Tonga	6.8	7.2	14	T77
12 DEC 1979	Colombia	6.4	7.7	17	
01 SEP 1981	Samoa	7.0	7.7	2	
19 DEC 1982	Tonga	5.9	7.7	2	T82
03 MAR 1985	Chile	6.7	7.8	10	
19 SEP 1985	Mexico	6.8	8.1	11	
07 MAY 1986	Aleutian Is.	6.4	7.7	13	
20 OCT 1986	Kermadec	6.6	8.1	8	
	Events used in present study				
02 SEP 1992	Nicaragua	5.3	7.2	3.4	N
12 DEC 1992	Flores Sea	6.5	7.5	5.1	F
12 JUL 1993	Hokkaido	6.7	7.6	4.7	Ho.
08 AUG 1993	Guam	7.2	8.1	5.2	G
21 JAN 1994	Halmahera	6.2	7.2	0.3	Ha.
02 JUN 1994	Java	5.5	7.2	3.5	J
04 OCT 1994	Kuriles	7.4	8.1	37	K
14 NOV 1994	Mindoro	6.0	7.1	0.59	M

provide some insight in at least two situations: when m_b fails to reach its saturation value, and when m_b, correctly measured at 1 s, exceeds the expected level of saturation (e.g., reaches values of 7 and above).

Figure 9, which plots seismic moment as a function of body-wave magnitude m_b for the eight earthquakes studied here, shows a significant deficiency of about 1 unit of magnitude in m_b for "tsunami earthquakes", relative to other earthquakes of the same moment. Both the Nicaragua and Java events have $m_b \leq 5.6$. The anomalous $m_b : M_0$ relationship results of course from the source duration of the earthquakes, which is much longer than the period of 1 s used to determine m_b.

We also added on this figure 13 other tsunamigenic events including the last two "tsunami earthquakes" of record prior to 1992 (Kuriles, June 10, 1975 and Tonga, December 19, 1982), as well as the great Tonga earthquake of June 22, 1977 (Table 4). All "tsunami earthquakes" are well separated from the regular tsunamigenic earthquakes, and conversely. Note in particular that PELAYO and WIENS (1992) had argued that the 1977 Tonga earthquake could have been regarded as exhibiting as $M_s : M_0$ discrepancy, and thus classified as a "tsunami earthquake," even though its tsunami was typical of its seismic moment (1.4×10^{21} N-m). However, LUNDGREN and OKAL (1989) showed that the event extended significantly at depth, thus explaining the M_s deficiency. Furthermore, there is no evidence of the $m_b : M_0$ deficiency that would be required by a slow source; on the contrary, large values of m_b could be an artifact of an inadequate depth correction: while 20-s excitation decreases substantially with depth below 60 km, body-wave magnitude corrections, as given by RICHTER (1958) are practically constant in that range of depths, and actually decrease for near-field ranges (corresponding to an increase of excitation).

Thus, the real-time analysis of a possible $m_b : M_0$ deficiency, through an automatic computation of m_b incorporated into the location algorithm could be useful as additional evidence confirming the "tsunami earthquake" character of an event.

Near-field Tsunami Warning Using TREMORS

The present study was motivated fundamentally by the ultimate purpose of all tsunami warning systems: that of providing an accurate warning in a time frame fast enough to allow the evacuation of people from low-lying areas. In the case of the Flores and Hokkaido tsunamis, the nearmost communities were hit by the tsunami two to five minutes after the origin time (H_0); this interval drops to maybe one or two minutes for Mindoro. In such situations, it is probably illusory to envision an efficient tsunami warning system, and only the alertness of the residents can save them, by running for high ground as soon as the shaking of the earthquake has died down: Figure 10 shows that the seismic moment reaches the warning threshold 4 minutes after the Hokkaido earthquake, and 10 minutes after the Flores one. Even if the stations were at closer epicentral distances, it takes at

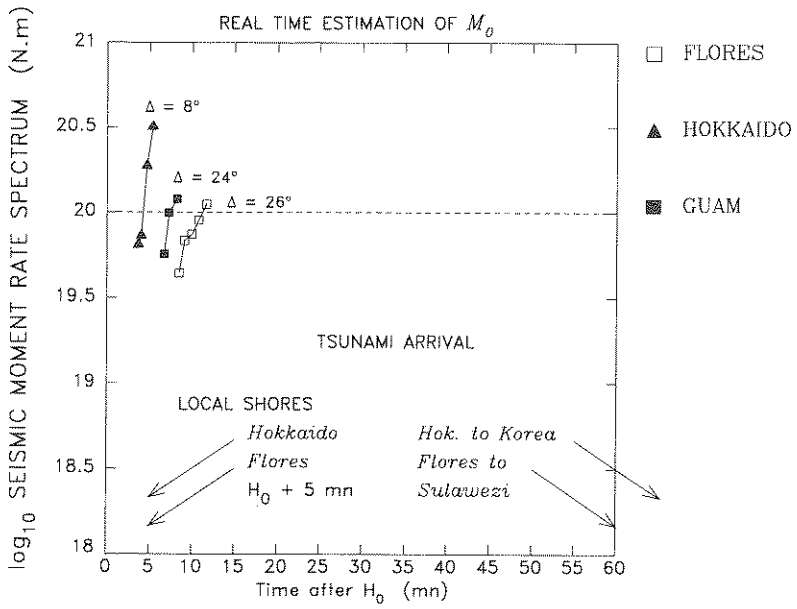

Figure 10

Real-time estimation of M_0 in the near field, in the case of the "fast" earthquakes (Flores and Hokkaido). On this figure (as on Figures 11 and 12), the various symbols show the estimates of the seismic moment rate spectrum obtained through the analysis of a growing window of seismic data, plotted as a function of time after H_0. The dashed line shows the moment threshold (10^{20} N-m) considered as representative as tsunami danger in the near field. A warning could have been issued as soon as M_0 reaches this threshold. Also indicated are the arrival times of the tsunami, both at the local shores, and at more distant locations. The Guam earthquake is also included for reference.

least 1 or 2 minutes to measure energy at frequencies lower than 20 mHz. With the rupture zones close to the coasts (possibly intersecting it in the case of Mindoro), early warning was impossible for the nearmost communities, but remains feasible for more distant locations, such as Honshu, Russia and Korea in the case of the Hokkaido event, and Sulawezi for the Flores one.

On the other hand, the Nicaragua and Java tsunamis, generated at the relatively distant trenches, hit the coast an average of 40 minutes after origin time. The Kuriles tsunami was generated closer than the trench, but in shallow seas, thereby slowing down its progression, and it reached Iturup and Kunashir 8 and 12 mn respectively after H_0.

The seismic moment of the Nicaraguan event exceeded 10^{20} N-m at the Mexican station UNM only 8 minutes after H_0. During the next 10 minutes, the crucial part of the Rayleigh waves (i.e., the long-period mantle waves) arrived, and it would have become possible to monitor the remarkable build-up of the seismic moment, and to detect the "tsunami earthquake" character of the event not more than 18 minutes after H_0 (Figure 11). Thus, a warning could have been issued for the

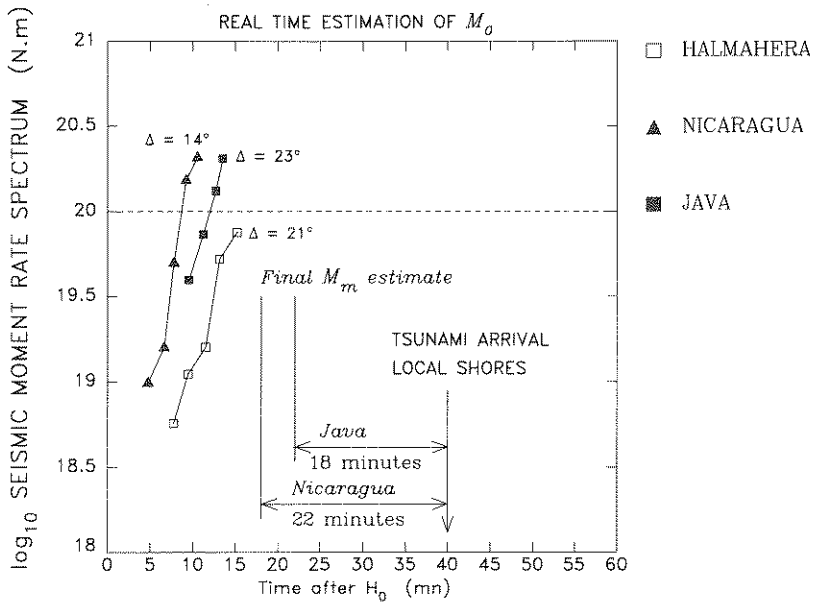

Figure 11

Same as Figure 10, for the "slow" events (or "tsunami earthquakes"). Note the spectacular increase (more than 1 order of magnitude) of the moment over about 5 mn in the case of Nicaragua, and a relatively similar situation for Java. The threshold is reached 7 and 11 mn respectively after H_0, with the final estimate of the mantle magnitude obtained about 20 mn after H_0, leaving adequate time before the arrival of the waves for these earthquakes, which occurred at the trench. In the case of Halmahera, there may be some evidence of a similar growth of the moment, but the final value fails to reach the threshold of danger.

Nicaraguan and Costa Rican coasts at least 22 minutes before the tsunami hit the coast. We recall that this earthquake was not even felt by residents of some sections of the coastline, who were to be swept away 40 minutes later.

In the case of the Java tsunami, the seismic moment exceeded 10^{20} N-m at station WRA 12 minutes after H_0. An efficient warning for Java residents could have been issued at least 18 minutes before the tsunami hit the coast.

In the case of the Kuriles tsunami, the very first estimate of the seismic moment, which can be obtained 4 minutes after H_0, is already 10 times the 10^{20} N-m threshold, and precedes the tsunami wave at Iturup by 4 minutes (Figure 12). While this lead time may be considered short, it increases to 8 minutes at Kunashir, and 20 minutes at Nemuro on the East coast of Hokkaido.

Conclusion

Our results show that TREMORS is indeed an efficient system for the rapid, automatic, estimation of the seismic moments of strong earthquakes both in the far

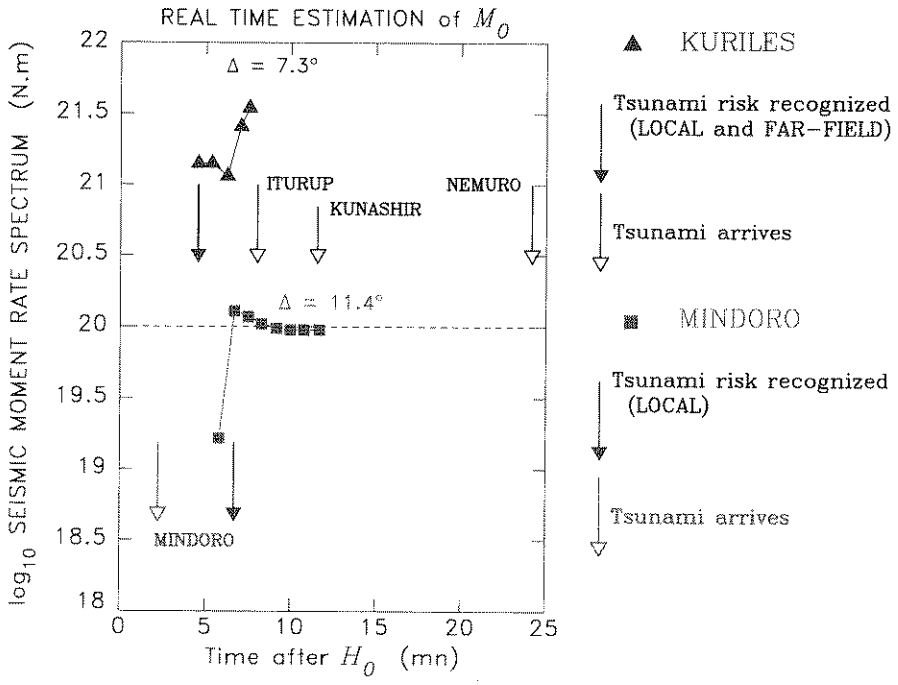

Figure 12

Same as Figure 10 for the more recent Kuriles and Mindoro events. In the case of Kuriles, note that the very first measurement is already considerably larger than the threshold of danger, which would warrant an immediate alarm, 4 mn after H_0. In the case of Mindoro, the alarm is also nearly immediate, but the station is clearly too distant to provide any efficient warning.

and near fields. As such, it can realistically be used as a reliable tsunami warning system. TREMORS can compute automatically an acceptable location, generate a warning in all the cases studied, except Halmahera, which is justified given both the smaller size of the earthquake, and the amplitude of the resulting tsunami, which incidentally did not cause any additional casualties or damage. Thus, our present experience suggests that a warning threshold of 10^{20} N-m seems an appropriate value in the near field for the generation of a dangerous tsunami. Our simulations obtained by computing seismic moments in windows of growing length, show that warnings would be issued within 4 to 11 minutes of H_0, depending on the epicentral distance, and that a final assessment of the seismic moment, including the possible recognition of "tsunami earthquake" character would be available within 18 to 20 minutes after H_0. In the case of a major earthquake, such as the Kuriles event, the warning is immediately available ($H_0 + 4$ minutes).

Unfortunately, at present, because of instrumental limitations, the traditional tsunami warning system continues to rely heavily on the 20-second M_s, a magnitude scale notoriously plagued by saturation effects in the precise range of earthquake sizes generating large tsunamis (GELLER, 1976; TALANDIER and OKAL, 1989). For

slow "tsunami earthquakes" such as the Nicaragua or Java events, the classical magnitudes do not represent the true tsunami potential of the event. On the other hand, TREMORS has the capability of recognizing these events in real time, and of giving a lead time of about 20 minutes in the case of earthquakes generated at the subduction trenches. We want to stress that these figures were obtained using relatively distant broadband stations, situated about 15° from the epicenters. Obviously, better results could be obtained with closer stations, as demonstrated by the AOB/Kuriles combination. However, we think that a reliable global tsunami warning system could be built around several regional centers equipped with such an automated intelligent system. Each center would be in charge of a seismic zone with a 15° radius. This approach, whose cost and logistics are much lower than traditional dense seismic networks, should be a significant step towards effective tsunami warning and hazard reduction.

Acknowledgments

We thank the GEOSCOPE and IRIS data centers for providing the broadband data and Göran Ekström for the most recent 1994 CMT solutions. We also thank our colleagues in the tsunami community for many discussions. This research is supported by Commissariat à l'Energie Atomique (France).

REFERENCES

DZIEWONSKI, A. M., EKSTRÖM, G., and SALGANIK, M. P. (1993a), *Centroid-moment Tensor Solutions for July-September 1992*, Phys. Earth. Planet. Inter. *79*, 287–297.

DZIEWONSKI, A. M., EKSTRÖM, G., and SALGANIK, M. P. (1993b), *Centroid-moment Tensor Solutions for October-December 1992*, Phys. Earth. Planet. Inter. *80*, 89–103.

DZIEWONSKI, A. M., EKSTRÖM, G., and SALGANIK, M. P. (1994a), *Centroid-moment Tensor Solutions for July-September 1993*, Phys. Earth. Planet. Inter. *83*, 165–174.

DZIEWONSKI, A. M., EKSTRÖM, G., and SALGANIK, M. P. (1994b), *Centroid-moment Tensor Solutions for January-March 1994*, Phys. Earth. Planet. Inter. *86*, 253–261.

FURUMOTO, A. S. (1993), *Three Deadly Tsunamis in One Year*, Science of Tsunami Hazards, 111–121.

GELLER, R. J. (1976), *Scaling Relations for Earthquake Source Parameters and Magnitudes*, Bull. Seismol. Soc. Am. *66*, 1501–1523.

HASKELL, N. A. (1962), *Crustal Reflection of Plane P and SV Waves*, J. Geophys. Res. *67*, 4751–4767.

HOKKAIDO TSUNAMI SURVEY GROUP (1993), *Tsunami Devastates Japanese Coastal Region*, EOS, Trans. Am. Geophys. Un. *74*, 417–432.

HYVERNAUD, O., REYMOND, D., TALANDIER, J., and OKAL, E. A. (1992), *Four Years of Automated Measurements of Seismic Moments of Papeete using the Mantle Magnitude* M_m: 1987–1991, Tectonophysics *217*, 175–193.

KANAMORI, H. (1972), *Mechanisms of Tsunami Earthquakes*, Phys. Earth. Planet. Inter. *6*, 346–359.

KANAMORI, H. (1977), *The Energy Release in Great Earthquakes*, J. Geophys. Res. *82*, 2981–2987.

KANAMORI, H., and KIKUCHI, M. (1993), *The 1992 Nicaragua Earthquake: A Slow Tsunami Earthquake Associated with Subducted Sediment*, Nature *361*, 714–715.

KAWATA, Y. (1993), *Response of Residents at the Moment of Tsunamis.—The 1992 Flores Island Earthquake Tsunami, Indonesia.* Proceedings of the IUGC/IOC International Tsunami Symposium, Wakayama, Japan, Aug. 23–27, 1993, pp. 677–688.

LASKE, G. (1995), *Global Observation of Off-great Circle Propagation of Long-period Surface Waves*, J. Geophys. Res., in press.

LUNDGREN, P. R., and OKAL, E. A. (1988), *Slab Decoupling in the Tonga Arc: The June 22, 1977 Earthquake*, J. Geophys. Res. *93*, 13355–13366.

NAKANISHI, I., KODAIRA, S., KOBAYASHI, R., KASAHARA, M., and KIKUCHI, M. (1993), *Quake and Tsunami Devastate Small Town*, EOS, Trans. Am. Geophys. Un. *74* (34), 377–379.

OKAL, E. A. (1988), *Seismic Parameters Controlling Far-field Tsunami Amplitudes: A Review*, Natural Hazards *1*, 67–96.

OKAL, E. A. (1989), *A Theoretical Discussion of Time-domain Magnitudes: The Prague Formula for M_s and the Mantle Magnitude M_m*, J. Geophys. Res. *94*, 4194–4204.

OKAL, E. A. (1990), *M_m: A Mantle Wave Magnitude for Intermediate and Deep Earthquakes*, Pure and Appl. Geophys. *134*, 333–354.

OKAL, E. A., and ROMANOWICZ, B. A. (1994), *On the Variation of b-value with Earthquake Size*, Phys. Earth Planet. Inter. *87*, 55–76.

OKAL, E. A., and TALANDIER, J. (1989), *M_m: A Variable-period Mantle Magnitude*, J. Geophys. Res. *94*, 4169–4193.

OKAL, E. A., and TALANDIER, J. (1990), *M_m: Extension to Love Waves of the Concept of a Variable-period Mantle Magnitude*, Pure and Appl. Geophys. *134*, 355–384.

PELAYO, A. M., and WIENS, D. A. (1992), *Tsunami Earthquakes: Slow Thrust-faulting Events in the Accretionary Wedge*, J. Geophys. Res. *97*, 15312–15337.

REYMOND, D., HYVERNAUD, O., and TALANDIER, J. (1991), *Automatic Detection, Location and Quantification of Earthquakes: Application to Tsunami Warning*, Pure and Appl. Geophys *135*, 361–382.

REYMOND, D., HYVERNAUD, O., and TALANDIER, J. (1993), *An Integrated System for Real-time Estimation of Seismic Source Parameters and its Application to Tsunami Warning*, Tsunami in the World, 177–196.

RICHTER, C. F., *Elementary Seismology* (W. H. Freeman, San Francisco, 1958).

ROMANOWICZ, B., CARA, M., FELS, J.-F., and ROULAND, D. (1984) GEOSCOPE: *A French Initiative in Long-period Three-component Global Seismic Networks*, EOS, Trans. Am. Geophys. Un. *65*, 753–754.

SATAKE, K., BOURGEOIS, J., ABE, KU., ABE, KA., TSUJI, Y., IMAMURA, F., IIO, Y., KATAO, H., NOGUERA, E., and ESTRADA, F. (1993), *Tsunami Field Survey of the 1992 Nicaragua Earthquake*, EOS, Trans. Am. Geophys. Un. *74*, 145 and 156–157, 1993.

SUNARJO, (1993), *Experience in Handling the Flores Earthquake-tsunami of Dec. 12, 1992*, Proceedings of the IUGC/IOC International Tsunami Symposium, Wakayama, Japan, Aug. 23–27, 1993, pp. 861–869.

TALANDIER, J. (1993), *French Polynesia Tsunami Warning Center (CPPT)*, Natural Hazards *7*, 237–256.

TALANDIER, J., and OKAL, E. A. (1992), *One Station Estimates of Seismic Moments from the Mantle Magnitude M_m: The Case of the Regional Field* ($1.5 \leq \Delta \leq 15°$), Pure and Appl. Geophys. *138*, 43–60.

TANIOKA, Y., RUFF, L. J., and SATAKE, K. (1993), *Unusual Rupture Process of the Japan Sea Earthquake*, EOS, Trans. Am. Geophys. Un. *74* (34), 377–380.

TANIOKA, Y., and SATAKE, K. (1994), *The 1994 Java Earthquake and Tsunami*, EOS, Trans. Am. Geophys. Un. *75* (44), 355–356 (abstract).

YEH, H. (1993), *Disaster on Flores Island*, Nature *361*, 686.

(Received September 1, 1994, revised January 21, 1995, accepted January 30, 1995)